Journal of Engineering and Technological Advances (JETA)
https://jeta.segi.edu.my/index.php/segi
2022 Vol. 7 No. 2

INFLUENCE OF OPERATING CONDITIONS ON THE ULTRAFILTRATION TREATMENT OF BRILLIANT BLUE *BATIK* DYE

Ho, K. C. *, Selvaraj, D.

Centre for Water Research, Faculty of Engineering, Built Environment and Information Technology, SEGi University, Jalan Teknologi, Kota Damansara, 47810 Petaling Jaya, Selangor Darul Ehsan, Malaysia

* Corresponding Author: hokahchun@segi.edu.my TEL: (603)-61451777

Abstract: The *batik* industry produces a large amount of wastewater that degrades water quality. Ultrafiltration (UF) is an efficient and low-pressure filtration method for water treatment, particularly for dye wastewater. This study aims to analyze the efficiency of commercial UF polyethersulfone (PES) membranes in the treatment of brilliant blue *batik* dye. The effect of operating conditions involving operating pressure (2, 3, 4 bar) and pH (3, 6, and 9) of dye solution at 50 mg/L on membrane performance was evaluated via a crossflow filtration system. Higher dye rejection was obtained at close to neutral pH and higher pressure. On the other hand, the fouling propensity was mainly affected by pressure and the membrane experienced a slower flux decline at lower pressure. This is owing to the synergistic interaction between size sieving and electrostatic repulsion. The optimum membrane performance was achieved at pH 6 and 3 bar. Future studies can work on real dye wastewater produced from the *batik* industry.

Keywords: Brilliant Blue *Batik* Dye; Ultrafiltration; Operating Conditions; pH; Pressure.

1. Introduction

The textile and apparel industry is a rapid-growing market, with China, European Union, India, and the United States as major competitors (Teow et al., 2020). Malaysia has also established itself as a global powerhouse in these sectors. *Batik* industry in Malaysia is considered a national heritage art produced through various textile designing techniques (Razali et al., 2021). The *batik* industry uses huge volume of water during production subsequently leads to the discharge of enormous wastewater (Faiza et al., 2022). The *batik* industry wastewater raises

concerns from authorities because the wastewater hardly fulfils standard sewage limit and regulations, which. *Batik* wastewater may impose environmental pollution and health issues (Rashidi et al., 2012). As the *batik* industry is typically operated by small family businesses, hence they usually discharge the untreated hazardous wastewater directly into water bodies.

In some *batik* premises in Malaysia, integrated system composed of sand filtration and activated carbon adsorption is employed for the wastewater treatment (Nuzul et al., 2020). However, this conventional treatment system is incapable to bring pollutant concentration in *batik* wastewater to the permissible limit (Mohamad Mazuki et al., 2020). Alternatively, membrane filtration has appeared to be a viable solution for treating *batik* industry wastewater because of its ease of use, cost-effectiveness, and high quality of treated water (Chen et al., 2022; Teow et al., 2022). Rashidi et al. (2012) have treated the synthetic wastewater from the *batik* industry using commercial nanofiltration membrane, NF TS80, Trisep. Dye rejection of 80.1-93.8% was reported after 45 minutes of filtration. Nevertheless, nanofiltration membranes require high operating cost and offer low permeability (Mohammad et al., 2018). Besides, membrane fouling remains a major issue of membrane technology (Lee et al., 2022).

Membrane operating conditions have a significant impact on the performance of membranes, particularly rejection and fouling tendency (Ren et al., 2019). The main driving force for solute permeation is the membrane operating pressure. A low operating pressure is found to consume lower energy, thus allowing smaller solutes to permeate through the membrane. On the contrary, high operating pressure causes concentration polarization and forces larger solutes through the membranes (Faneer et al., 2017). In addition, the interaction of solutes with membrane surfaces can affect filtration performance. The electrostatic repulsion between the membrane surface charge and dye could influence the retention of solutes. For instance, Kolangare et al. (2019) reported that the electrostatic attraction between a positively charged chitosan membrane and the negatively charged dye affects the rejection of dye molecules.

Throughout the study, a commercial ultrafiltration (UF) polyethersulfone (PES) membrane was employed to treat *batik* industry synthetic wastewater. Brilliant Blue *batik* dye was used to produce synthetic wastewater. The influence of operating conditions i.e. operating pressure and pH of dye solution on membrane performance was evaluated via a crossflow filtration system.

2. Materials and Methods

2.1. Materials

Commercial UF PES flat sheet membrane, UF10, with nominal MWCO of 10 kDa was supplied by TriSep, USA. The maximum operating pressure and pH range of the UF10 membrane are 21 bar and 2-11, respectively. Brilliant Blue *batik* powder dye was purchased from Multifilla (M) Sdn. Bhd., Malaysia. Dye solutions were prepared by dissolving Brilliant Blue *batik* powder dye in reverse osmosis (RO) water. The pH of dye solutions was altered with hydrochloric acid (HCl) and sodium hydroxide (NaOH), supplied by R&M Chemicals, UK.

2.2. Membrane Characterization

The functional groups on the UF PES membrane were analyzed by Spectrum 100, PerkinElmer, UK. The membrane flux was measured in a lab-scale crossflow filtration system with a total effective membrane area of 19.6 cm^2. Prior to testing, the UF PES membrane was compressed for 20 minutes under 5 bar of RO water to minimize the effects of deformation on the membrane (Yadak Yaraghi et al., 2022). Membrane flux was measured at a pressure of 2, 3, and 4 bar and computed using Equation 1.

$$J = \frac{V}{A \times t} \quad (1)$$

where J is permeation flux (L $m^{-2}h^{-1}$), V is the volume of the permeate (L), t is time to collect the permeate (h), and A is an area of the effective membrane area (m^2)

2.3. Effect of Operating Conditions

Membrane performance including dye rejection and fouling propensity was evaluated using a similar lab-scale crossflow filtration system (Figure 1). The Brilliant Blue *batik* dye solution with fixed concentration of 50 mg/L was utilized as the feed solution (Ho et al., 2022). Membrane operating pressure was varied at 2, 3, and 4 bar while the pH of the dye solution was varied at 3, 6, and 9 with the aid of HCl and NaOH. Dye concentrations in permeate were determined at 570 nm using a UV-1900 spectrophotometer, Shimadzu, Japan (Syafiuddin & Fulazzaky, 2021). Dye rejection was measured at an interval of 10 minutes for 60 minutes of filtration and calculated using Equation 2. Fouling propensity was represented by normalized flux determined using Equation 3.

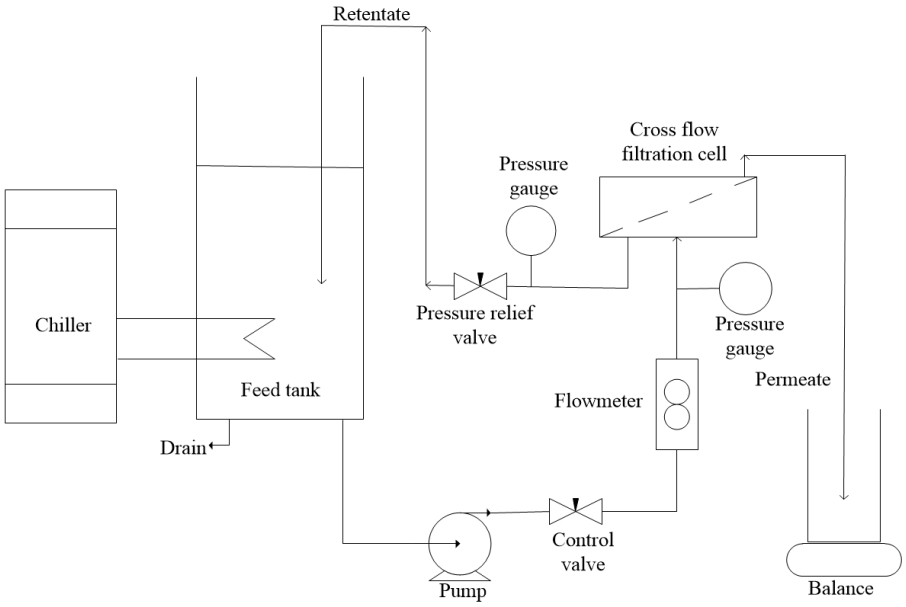

Figure 1. Schematic diagram of lab-scale crossflow filtration system

$$R\% = (1 - \frac{C_p}{C_f}) \times 100 \quad (2)$$

where C_f is the concentration of dye in the feed solution (mg/L), C_p is the concentration of dye in permeate solution (mg/L) and R is dye rejection (%)

$$Normalized\ flux = \frac{J_1}{J} \quad (3)$$

where J_1 is permeate flux and J = RO water flux

3. Results and Discussion

3.1. Membrane Characterization

Figure 2 depicts FTIR spectroscopy for pristine UF PES membrane and tested UF PES membrane at pH 3. As seen, UF PES membrane contains band at 3400 cm^{-1} (OH stretch) and two bands at 1650 cm^{-1} (C=O stretching) and 1040 cm^{-1} (asymmetric and symmetric vibrations of SO_3^-) (Zhu et al., 2015). The tested UF PES membranes exhibit more intense peaks at 3400 cm^{-1} and 1650 cm^{-1} attributed to O-H stretching of hydroxyl group as well as C=O stretching in carboxylic anhydride, ketone, and lactone respectively (Ahmad et al., 2020). These are attributed to the adsorption of Brilliant Blue *batik* dye on the membrane surface by the broad

overlapping absorption band (3448.31 cm^{-1}), suggested N-H and O-H stretching vibrations (Syafiuddin & Fulazzaky, 2021).

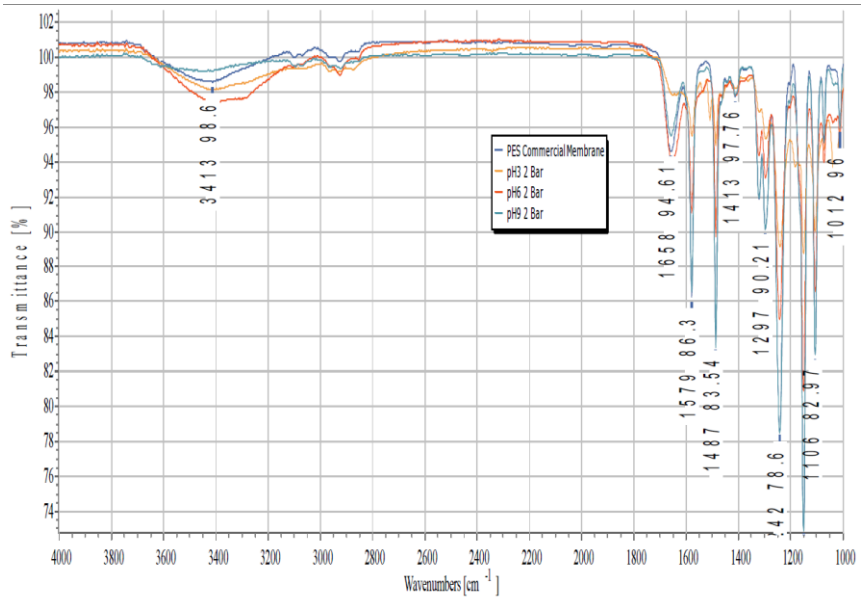

Figure 2. FTIR spectroscopy of membranes

Table 1 shows membrane water permeation flux at 2, 3, and 4 bar. The increase of the pressure increases the permeation drag force forward the membrane surface hence higher the permeate flux (Echakouri et al., 2022). The average membrane water permeability with the reference to the permeate flux at a specific pressure is 78.26±8.44 L $m^{-2}h^{-1}bar^{-1}$ which is close to the specification given by the manufacturer (74 L $m^{-2}h^{-1}bar^{-1}$).

Table 1. Membrane water permeation flux

Pressure (bar)	Permeation flux (L $m^{-2}h^{-1}$)
2	146.68±5.76
3	213.90±2.50
4	360.58±16.23

3.2. Effect of Operating Conditions on Membrane Performance

3.2.1. Dye Rejection

Figure 3 represents the dye rejection for the UF PES membrane at the operating pressure of 2, 3, and 4 bars. It shows that the membrane has a relatively stable performance. Initially, the dye rejection ranges between 93.55-97.74 % and decreases to 87.10-97.10 % over time. This is because of the dye adsorption on the membrane surface during the filtration process,

subsequently deteriorates the membrane capacity. This is in accordance to a study by Abdi et al. (2018) where the copper ion rejection by the PES membrane decreased by around 2-5% after each run of the experiment. In general, higher dye rejection was obtained at close to neutral pH and higher pressure. Whereas, lower dye rejection was achieved at acidic pH and lower pressure.

At constant pH, increasing the pressure will improve the dye rejection. For instance, at a pH of 6, the dye rejection increases from 93.87-96.45 % (2 bar) to 95.16-96.77 % (3 bar). This is attributed to the intensified dilution effect which lowers the effective dye concentration in the permeate by higher water flux at elevated pressure (Ye et al., 2018). The same trend was also observed at pH 3 and pH 9. It is emphasized in the literature that the rejection of salt increases with increasing pressure primarily owing to the membrane compaction, whilst a gradual drop beyond 6 bar because of high hoop stress on the inner dense-selective layer of the membrane (Han et al., 2018).

At constant pressure, the dye rejection performance of the UF PES membrane is comparatively stable at pH 6. The dye rejection at pH 6 fluctuates in a small range at 93.87-96.45 %, 95.16-96.77 %, and 95.16-96.77 % at a pressure of 2, 3, and 4 bar, respectively. This is because under close to neutral environments, strong and stable dye aggregates were produced via hydrophobic interactions between the dyes. This increases the effective size of the dye and subsequently improves the dye rejection by size exclusion mechanism. This is in accordance with Moradi et al. (2020) where the rejection of Direct red 16 was relatively stable at pH 4 and 6 but decreased when the pH was increased to 10. Besides, increasing the pH also increases the electrostatic repulsion between the negatively charged dye and likewise membrane surface. This is observed at a higher pressure of 3 and 4 bar. The dye rejection increased gradually from 95.16-96.77 % (pH 6) to 97.10-97.74 % (pH 9) at 3 bar. It was also observed by other studies that the rejection of anionic dyes increased when the membrane presented with a negative charge caused by the strong electrostatic repulsion (Fang et al., 2020). Therefore, the rejection of dyes is attributed to the combined interaction of size sieving and electrostatic repulsion.

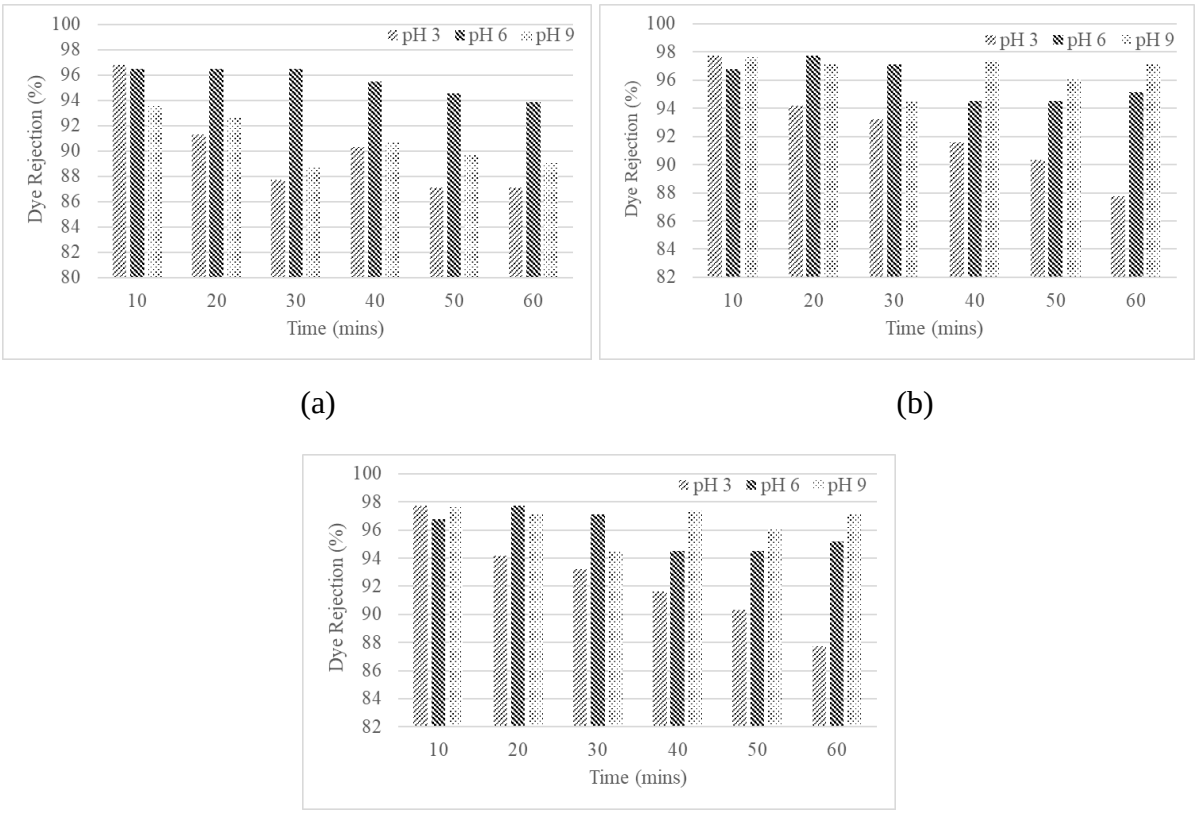

Figure 3. Dye rejection at (a) 2, (b) 3, and (c) 4 bar

3.2.2. Fouling Propensity

The fouling propensity of the membrane was represented by normalized flux. High normalized flux indicates better membrane fouling propensity. The normalized flux of the UF PES membrane at 2, 3, and 4 bars is shown in Figure 4. In general, the normalized flux of the membrane decreases over time. This is caused by the dye molecule adsorption on membrane surfaces, as well as pore blockage or plugging over long period of filtration. Consequently, this results in the declination of water movement across the membrane. As observed in Figure 4, the fouling propensity is mainly affected by pressure, and the membrane experience a slower flux decline at lower pressure.

At constant pH, increasing the pressure will result in rapid flux decline. For instance, at a pH of 6, the normalized flux decreased by 17.70 % and 31.90 % when the pressure raised from 2 bar to 3 bar. This is attributed to high permeation drag and driving force at high pressure. This resulted in cake formation on membrane hence rapid flux decline. Same trend was observed at pH 9. The normalized flux decreased by 37.00 % and 64.30 % when the pressure increased from 3 bar to 4 bar. Wang et al. (2018) observed a higher flux decline during filtration using

methyl green solution (50 mg/L) due to the increased osmotic pressure in the presence of salt in solution. Besides, the severe flux decline was also reported with increasing osmotic pressure in dye-salt solution due to the cake-enhanced concentration polarization (Ye et al., 2018).

At constant pressure, the fouling propensity performance of UF PES membrane is relatively stable at pH 9 except at high pressure. The normalized flux after 60 minutes of filtration at pH 9 ranges is 0.829, 0.630, and 0.357 at 2 bar, 3 bar, and 4 bar, respectively. This is because the membrane has turned to be negatively charged caused by the addition of NaOH during pH adjustment. This has increased hydroxyl ion adsorption and negative ions density on the membrane surface. This enhances the electrical repulsive force between the negatively charged dyes and the membrane surfaces. Subsequently, the concentration polarization effect and the dye adsorption on the membrane surface are reduced. Therefore, the membrane can withstand greater flux than that of lower pH. Xing et al. (2015) reported that electrostatic repulsion force between negatively charged solutes and membrane surface has direct effect on fouling propensity. However, the normalized flux with a feed pH of 9 at 4 bar was relatively low due to severe membrane fouling. This signified that increasing operating pressure speeds up the formation of cake layer awing to high permeation drag. The cake layer increases the membrane resistance and reduces the flux significantly (Zhou et al., 2021).

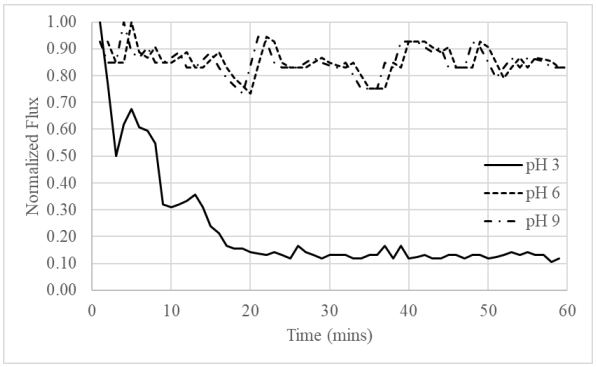

(a)

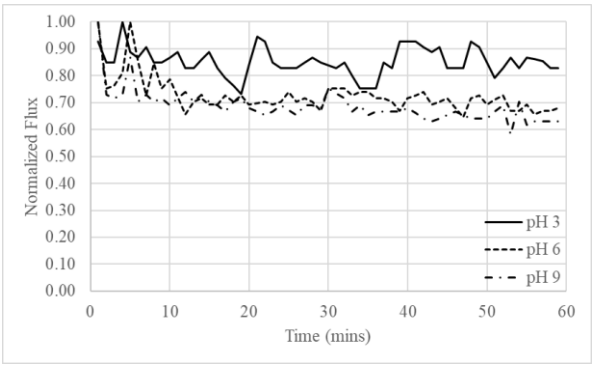

(b)

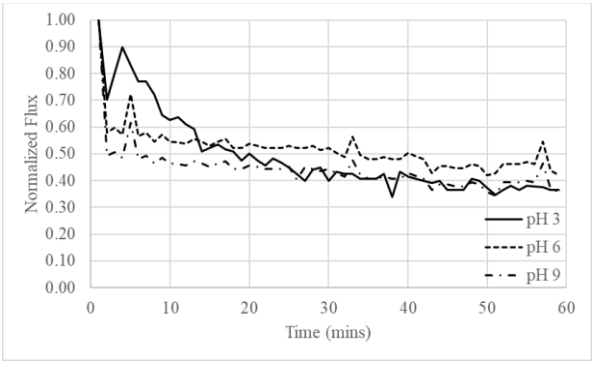

(c)

Figure 4. Normalized flux at (a) 2, (b) 3, and (c) 4 bar

4. Conclusion

In conclusion, the effect of operating conditions (pressure and pH) on the UF treatment of brilliant blue *batik* dye has been investigated. The transmembrane pressure was varied at 2, 3, and 4 bar, while the pH of the dye solution was manipulated at 3, 6, and 9. The optimum membrane performance was achieved at pH 6 and 3 bar because of the synergistic effect of size exclusion and electrostatic interaction between dyes and membrane surface. Research findings suggested that higher dye rejection was obtained at close to neutral pH and higher pressure. This is because of the formation of strong and stable dye aggregates and enhanced dilution effect at higher pressures. On the contrary, the fouling propensity was mainly affected by pressure, and the membrane experienced a slower flux decline at lower pressure. This is attributed to the lower concentration polarization effect, reducing dye adsorption on the membrane surface at low pressure. Future studies can work on real dye wastewater generated by the *batik* industry, as the performance of the membrane can be affected by other types of dyes and pollutants in the real samples.

Acknowledgement

This research is fully supported by SEGi Internal Research Fund grant, SEGiIRF/2022-Q1/FoEBEIT/002.

References

Abdi, G., Alizadeh, A., Zinadini, S., & Moradi, G. (2018). Removal of dye and heavy metal ion using a novel synthetic polyethersulfone nanofiltration membrane modified by magnetic graphene oxide/metformin hybrid. *Journal of Membrane Science, 552*, 326–335.

Ahmad, M. A., Eusoff, M. A., Oladoye, P. O., Adegoke, K. A., & Bello, O. S. (2020). Statistical optimization of Remazol Brilliant Blue R dye adsorption onto activated carbon prepared from pomegranate fruit peel. *Chemical Data Collections*, *28*, 100426.

Chen, Y. M., Kah Chun, H., Chan, M. K., Teow, Y. H., & Aida Isma, M. (2022). Optimization of Antifouling Properties of Mixed Matrix Membrane Synthesized via in-situ Colloidal Precipitation. *Journal of Membrane Science and Research*. 9, 557323

Echakouri, M., Salama, A., & Henni, A. (2022). Experimental Investigation of the Novel Periodic Feed Pressure Technique in Minimizing Fouling during the Filtration of Oily Water Systems Using Ceramic Membranes. *Membranes*, *12*(9), 868.

Faiza, N., Vin Cent, T., & Munira, M. (2022). Trend Analysis of River Flow In Langat River Basin Using Swat Model. *Journal of Engineering & Technological Advances*, *7*(1). 13 - 22

Faneer, K. A., Rohani, R., Mohammad, A. W., & Ba-Abbad, M. M. (2017). Evaluation of the operating parameters for the separation of xylitol from a mixed sugar solution by using a

polyethersulfone nanofiltration membrane. *Korean Journal of Chemical Engineering*, *34*(11), 2944–2957.

Fang, S. Y., Zhang, P., Gong, J. L., Tang, L., Zeng, G. M., Song, B., Cao, W. C., Li, J., & Ye, J. (2020). Construction of highly water-stable metal-organic framework UiO-66 thin-film composite membrane for dyes and antibiotics separation. *Chemical Engineering Journal*, *385*.

Han, G., Chung, T.-S., Weber, M., & Maletzko, C. (2018). Low-Pressure Nanofiltration Hollow Fiber Membranes for Effective Fractionation of Dyes and Inorganic Salts in Textile Wastewater. *Environmental Science & Technology*, *52*(6), 3676–3684.

Ho, K. C., Raffi, S. M., & Teow, Y. H. (2022). Synthesis of MWCNTs/TiO2 Photocatalytic Nanocomposite Membrane via In-situ Colloidal Precipitation Method for Methyl Orange Removal. *International Journal of Nanoelectronics and Materials*, *15*(3), 207–222.

Kolangare, I. M., Isloor, A. M., Karim, Z. A., Kulal, A., Ismail, A. F., Inamuddin, & Asiri, A. M. (2019). Antibiofouling hollow-fiber membranes for dye rejection by embedding chitosan and silver-loaded chitosan nanoparticles. *Environmental Chemistry Letters*, *17*(1), 581–587.

Lee, C. Z., Kah Chun, H., Chan, M. K., & Teow, Y. H. (2022). Effect of Carbon Nanomaterials Concentration in Nanocomposite Membrane for Methyl Blue Dye Removal. *Jurnal Teknologi*, *84*(6), 19–27.

Mohamad Mazuki, N. I., Teow, Y. H., Ho, K. C., & Mohammad, A. W. (2020). Techno-economic analysis of single disinfection units and integrated disinfection systems for sewage effluent reclamation. *Journal of Water Process Engineering*, *36*. 101398

Mohammad, A. W., Teow, Y. H., Ho, K. C., & Rosnan, N. A. (2018). Recent Developments in Nanofiltration for Food Applications. *Nanomaterials for Food Applications*, 101–120.

Moradi, G., Zinadini, S., & Rajabi, L. (2020). Development of high flux nanofiltration membrane using para-amino benzoate ferroxane nanoparticle for enhanced antifouling behavior and dye removal. *Process Safety and Environmental Protection*, *144*, 65–78.

Nuzul, Z., Talib, S. N., & Wan Johari, W. L. (2020). Water quality of effluent treatment systems from local batik industries. *IOP Conference Series: Earth and Environmental Science*, *476*(1), 012097.

Rashidi, H. R., Sulaiman, N. M. N., & Hashim, N. A. (2012). Batik Industry Synthetic Wastewater Treatment Using Nanofiltration Membrane. *Procedia Engineering*, *44*, 2010–2012.

Razali, H. M., Ibrahim, M., Omar, M., & Hashim, S. F. M. (2021). *Current challenges of the batik industry in Malaysia and proposed solutions*. 020269.

Ren, L., Yu, S., Li, J., & Li, L. (2019). Pilot study on the effects of operating parameters on membrane fouling during ultrafiltration of alkali/surfactant/polymer flooding wastewater: optimization and modeling. *RSC Advances*, *9*(20), 11111–11122.

Syafiuddin, A., & Fulazzaky, M. A. (2021). Decolorization kinetics and mass transfer mechanisms of Remazol Brilliant Blue R dye mediated by different fungi. *Biotechnology Reports*, *29*, e00573.

Teow, Y. H., Chiah, Y. H., Ho, K. C., & Mahmoudi, E. (2022). Treatment of semiconductor-industry wastewater with the application of ceramic membrane and polymeric membrane. *Journal of Cleaner Production*, *337*. 130569

Teow, Y. H., Tajudin, S. 'Aisyah, Ho, K. C., & Mohammad, A. W. (2020). Synthesis and characterization of graphene shell composite from oil palm frond juice for the treatment of dye-containing wastewater. *Journal of Water Process Engineering*, *35*.101185

Wang, X., Ju, X., Jia, T.-Z., Xia, Q.-C., Guo, J.-L., Wang, C., Cui, Z., Wang, Y., Xing, W., & Sun, S.-P. (2018). New surface cross-linking method to fabricate positively charged nanofiltration membranes for dye removal. *Journal of Chemical Technology & Biotechnology*, *93*(8), 2281–2291.

Xing, L., Guo, N., Zhang, Y., Zhang, H., & Liu, J. (2015). A negatively charged loose nanofiltration membrane by blending with poly (sodium 4-styrene sulfonate) grafted SiO2 via SI-ATRP for dye purification. *Separation and Purification Technology*, *146*, 50–59.

Yadak Yaraghi, A. H., Ramezanianpour, A. M., Ramezanianpour, A. A., Bahman-Zadeh, F., & Zolfagharnasab, A. (2022). Evaluation of test procedures for durability and permeability assessment of concretes containing calcined clay. *Journal of Building Engineering*, *58*, 105016.

Ye, W., Lin, J., Borrego, R., Chen, D., Sotto, A., Luis, P., Liu, M., Zhao, S., Tang, C. Y., & van der Bruggen, B. (2018). Advanced desalination of dye/NaCl mixures by a loose nanofiltration membrane for digital ink-jet printing. *Separation and Purification Technology*, *197*, 27–35.

Zhou, L., Xiao, G., He, Y., Wu, J., Shi, H., Zhong, F., Yin, X., Li, Z., & Chen, J. (2021). Multifunctional filtration membrane with anti-viscous-oils-fouling capacity and selective dyes adsorption ability for complex wastewater remediation. *Journal of Hazardous Materials*, *413*, 125379.

Zhu, S., Shi, M., Zhao, S., Wang, Z., Wang, J., & Wang, S. (2015). Preparation and characterization of a polyethersulfone/polyaniline nanocomposite membrane for ultrafiltration and as a substrate for a gas separation membrane. *RSC Advances*, *5*(34), 27211–27223.